Available online at www.sciencedirect.com
ScienceDirect
Renewable Energy 33 (2008) 1637–1651
RENEWABLE ENERGY
www.elsevier.com/locate/renene

Development of small domestic wind turbine with scoop and prediction of its annual power output

F. Wang[a,*], L. Bai[a], J. Fletcher[b], J. Whiteford[c], D. Cullen[c]

[a]School of Built Environment, Heriot-Watt University, EH14 4AS Edinburgh, UK
[b]School of Engineering and Physics Sciences, Heriot-Watt University, EH14 4AS Edinburgh, UK
[c]Dynamic Wind Generators Ltd, Fife, UK

Received 14 December 2006; accepted 15 August 2007
Available online 17 October 2007

Abstract

Based on an unperturbed airflow assumption and using a set of validated modelling methods, a series of activities were carried out to optimise an aerodynamic design of a small wind turbine for a built up area, where wind is significantly weaker and more turbulent than those open sites preferable for wind farms. These activities includes design of the blades using a FORTRAN code; design of the nose cones and nacelles, which then constituted the rotor along with the blades; optimisation of the rotor designs in the virtual wind tunnel developed in the first part of the study; and finally, estimation of the annual power output of this wind turbine calculated using hourly wind data of a real Scottish Weather Station. The predicted annual output of the finalised rotor was then compared with other commercial turbines and result was rather competitive.
© 2007 Elsevier Ltd. All rights reserved.

Keywords: Blade design; Blade element momentum (BEM); Computational fluid dynamics (CFD); Virtual wind tunnel; Power output

1. Introduction

The growing awareness of global warming and promotion on harnessing renewables have led wind turbines expanding from their preferable open sites into built up areas, where wind is significantly weaker and more turbulent than that in an open field. Although their environment benefits seem obvious, many concerns associated with this expending, such as predicting the actual energy yield of these wind turbines in an urban environment have been identified to be a serious matter to be resolved before to quantify their economical impacts [1,2]. On technical side, the increasing demand of efficient wind turbines has led to the development of numerous wind turbines that would work better in built environments. Part from improving electricity generation, storage and other efforts, increasing the airflow that drives rotor has been an effective measure to harness the available wind, for example, adding a wind scoop to collect more incoming flow (Fig. 1) or a diffuser to minimise the effects of wakes after rotor blades [3]. Many of such exploratory attempts have been assisted by aerodynamic analysis models developed to test the wind turbine in design stages. Various methods are available to calculate the aerodynamic forces on the blades of a horizontal axis wind turbine (HAWT), such as blade element momentum (BEM) method, lifting line method (LLM), lifting surfaces method (LSM), N–body/particle simulation methods, asymtotic expansion method (Euler special), Navier–Stokes equations [4]. Among them, BEM method seems the simplest and the most commonly used one to calculate the aerodynamic forces on wind turbine blades. Firstly proposed by Rankine [5] and Froude [6] in their pioneering work on propellers, and then developed by Lanchester [7], Betz [8] and Glauert [9], this method is based on an extension of actuator disk theory, applying the momentum method to an annular section stream tube around the rotor main axis, combined with blade forces obtained from aerodynamic tables as function of local inflow quantities. On the other side of the range, the Navier–Stokes equations method, appears elaborate and general as it resolves the set of equations

*Corresponding author. Tel.: +44 1314494636; fax: +44 1314513161.
E-mail address: fan.wang@hw.ac.uk (F. Wang).

0960-1481/$ - see front matter © 2007 Elsevier Ltd. All rights reserved.
doi:10.1016/j.renene.2007.08.008

Nomenclature

a	axial induction factor
a'	rotational induction factor
B	number of blades
c	chord
C_d	drag ratio, $C_d = D/(1/2\rho U_0^2 c)$
C_l	lift ratio, $C_l = L/(1/2\rho U_0^2 c)$
Cp	power coefficient, $C_p = P/(1/2\rho U_0^3 \pi R^2)$
D	drag per unit span
L	lift per unit span
P	power output
r	local radius
R	tip radius
U_T	rotational velocity on blade
U_P	axial velocity on blade
U_0	upstream undisturbed wind speed
W	relative wind speed
α	angle of attack
θ	blade angle
λ	tip speed ratio, $\lambda = \Omega R/U_0$
λ_r	local tip speed ratio, $\lambda_r = \Omega r/U_0$
σ	solidity, $\sigma = Bc/(2\pi R)$
φ	angle of the relative wind
Ω	angular velocity

which can capture both viscous and compressible effects for the global flow around the rotor as well as the local flows near the blades. As a result, the computed values are handily available for all the variables of the flow field [10,11]. It was this feature that made it the tool to predict the power output for this study, where the scoop was believed to have altered significantly the flow region around the rotor and its blades. The BEM was used to design the blade.

The main task in the aerodynamic analyses is optimising the design parameters to improve the performance of the rotor. While the performance of a rotor could be assessed in many ways, this study focused on its power output under a constant wind speed. Similarly the design parameters also could cover a wide range of option, from size to geometric details. This study was confined within a few that are commonly believed to be most influential to aerodynamic of the rotor, such as the number of blades; rotor solidity; pitch of blade; and tip speed ratio.

Previous studies [12–15] have investigated the implications of the solidity σ and number of blades on the power coefficient of a wind turbine. Duquette [12] carried out both the numerical and experimental studies of the number of blades and the solidity on the wind turbine with flat-plate, constant-chord blade sets and optimum-designed blade sets. Their study reveals that the increase of the solidity increases the power coefficient C_p. The experimental results from wind tunnel agree with this numerical result with regard to the solidity: C_p increases when the solidities of a three-bladed rotor increase from 14% to 27%. Furthermore, in conjunction with this increased power coefficient, is a reduction in tip speed ratio at maximum C_p. This finding is further supported by Nybroe's tests for a rotor of 3.8 m diameter [16]. This twelve-bladed windflower turbine can operate at a competitive power coefficient C_p, while at a much lower tip speed ratio than its counterparts.

But the effects of the number of blades on the power coefficient is not as consistent as what as been discussed above. Increasing the number of blades can increase the power coefficient, which is found in Duquette numerical results [12]. A contradictory has been revealed in wind

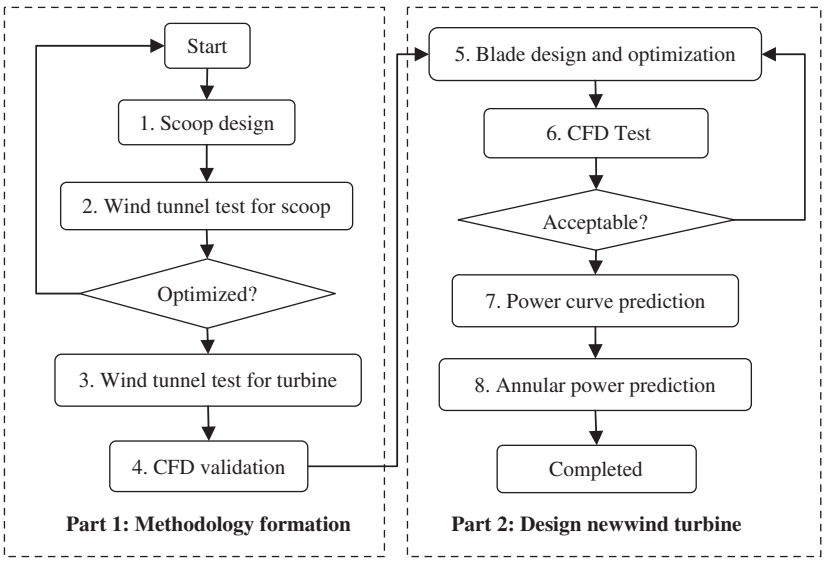

Fig. 1. Flowchart of the methodology used for the whole study project.

tunnel tests [13]. So far no literature has been found to explain such inconsistency between the two approaches. Therefore the number of blades and solidity of rotor was not included in the parameters to be examined.

One of the major problems for the small wind turbines is small torque that results in difficulty to start rotating in low wind speed [17,18]. There are normally several ways of solving this problem. The one adopted here was to use more blades, as this could add more torque to help start the wind turbine. Although they are harder to balance and yaw, rotors with more blades have strong twist at the ends of the blades and hence provides a big starting torque to start. The characteristics of being able to start rotating at low wind speed is very desirable for small wind turbines, as they are most likely to be installed in built up areas, where slow winds are dominant. Moreover, there was a six-blade test wind turbine readily available from a previous study. Therefore the new rotor had six blades, the same number as the one used in a previous study which was to first develop and then validate a systematic method based on computational fluid dynamics (CFD) modelling [19].

It has to be pointed out that the development and validation of the computational modelling approach was based on a simplification assumption of all modelling exercises: stable flow that was unperturbed in an open space, even though the scoop was expected to assist the wind turbine to work better in unstable winds in a built environment with many large obstructions. This assumption was made due to two limitations. Firstly in the wind tunnel where the real size wind turbine and scoop were tested, it was impossible to recreate the similar turbulent structure and the vortices as of those generated by the real buildings. Secondly it was again impossible to define the boundary conditions at the inlet of the CFD model to simulate such unstable features of the incoming wind to the wind turbine. Therefore the optimisation of the blades and other elements of the wind turbine were all based on this steady flow assumption.

So far literatures could not be found on the topic of blade design suitable for the diffuser-augmented wind turbine. Most studies are concentrated on the investigation of the diffuser itself [20–24]. Phillips et al. [25] tested diffuser-augmented wind turbine by varying one parameter at a time to assess the importance of each parameter, e.g. blade pitch, tip speed ratio, rotor solidity, tip clearance, etc. These results were used to determine the design configuration of the wind turbine that provided the greatest power output. Thus the rotor blades design had to rely on the BEM theory for conventional wind turbines in this study. The design speed in this exercise was taken as the speed that had been accelerated by the scoop, which was calculated using the steady flow assumption.

This paper presents the second part of the project on development of a small domestic wind turbine: a modelling study on a number of key design parameters of the turbine aerodynamics, which is outlined as follows: BEM theory was employed to design the new blades, and the rotor design was optimised by the CFD methods. The CFD method was used to compute the flow field of the computational domain that was considered large enough to minimise the effects of imposing boundary conditions. Being capable of providing flow details around all parts of the rotor, the CFD modelling was therefore used as a virtual wind tunnel for a parametric study to test various design options, for the shape of the blades and the rotor. Details of the overall design procedure are described in Section 2, including rotor design and annular power output calculation. The numerical method on which the virtual wind tunnel modelling was based is presented in Section 3. The results and discussions are given in Section 4 and conclusions are summarised in the last Section.

2. The design methods

The flowchart in Fig. 2 shows the overall structure of the project, consisting of 8 steps of activities. Whilst the Activities 1–4 that have been reported in [19] formed the first part of the project, it resulted in a validated method of CFD model that could be used to predict the power output of a turbine under a given condition. Built upon this virtual wind tunnel, this part of study that consisted of Activities 5–8 of which the objective was to design a new rotor that could perform better at low wind speeds and to estimate the annual power output of this final design.

More specifically, Activities 5 and 6 were to find an optimised design of the rotor at low speed, consisting of the blades, nose cone and nacelle. The blade shape was to be designed using BEM theory. The power performance was to be predicted by a CFD model developed using the method established in the first part of the study.

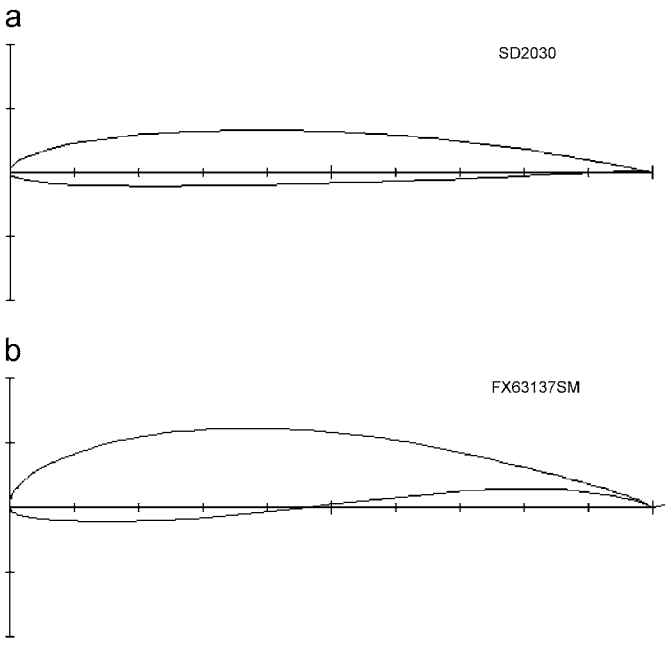

Fig. 2. The profiles of the two foils tested in this study. (a) Airfoil SD2030; (b) Airfoil FX63-137.

Activities 7 and 8 were to predict the annual power output of the finalised design using the predicted power curves obtained in Activity 6 and statistical wind data from Edinburgh, where hourly wind speeds were counted to calculate the cumulated power production of the turbine.

2.1. Rotor design

To optimise the aerodynamic performance of small wind turbines, the design of the rotor was considered to be the primary task at this stage, where a series of individual designs for the blades, nose cone & nacelle and combination of these elements together were to be tested. This task was to improve the power coefficient at a lower tip speed ratio through the use of more blades, large solidity and optimised blade pitch. Hence the rotor had six blades, slightly more than those products available at the market.

2.1.1. Airfoil selection

The aerodynamic and aeroacoustic characteristics for the small wind turbine are two major considerations in the process of selecting an airfoil. To produce a quiet and efficient small wind turbine, the results [26–28] from wind tunnel tests carried out by National Renewable Energy Laboratory (NREL) were used to select a suitable airfoil. In the NREL's report, they have tested six kinds of airfoils for use on small wind turbines. FX 63-137 and SD2030 were to be assessed in this study as they were the only two unpatented at the time.

Originally designed for human-powered aircraft, FX 63-137 has been used for many applications with low Reynolds number due to its high-lift, soft-stall characteristics, such as small wind turbines Lakota (Aeromag), H-40 and H-80 (Southwest Windpower). The other airfoil, SD2030, originally designed for model sailplanes (Fig. 3(a)), has been widely used for small wind turbines, including Southwest Windpower's small wind turbines, Air 403 and Air X. Compared with the FX 63-137, this airfoil has quite low drag at the expense of a narrower drag polar. This low drag is achieved by having a long transition ramp, or "bubble ramp" that leads to a thin laminar separation bubble [28]. As deduced from the high camber, airfoil FX 63-137 (Fig. 3(b)) should be able to produce considerably more lift than the SD2030. However, FX63-137 suffers the consequences of a large laminar separation bubble, at $Re = 100{,}000$.

Aeroacoustic characteristics were also considered in the process of selecting the right airfoil for the blades, although not included as one of the parameters being examined in this study. Taken into account were three key aeroacoustic sound levels: the trailing edge noise, weighted overall trailing edge noise, and overall inflow turbulence noise at $32\,\mathrm{m\,s^{-1}}$, which were from a study conducted for six airfoils including the two discussed here at higher Reynolds number than ours. [21].

To conclude, SD2030 was eventually selected for this study and FX63-137 was dropped for its laminar separation issue of airfoil and relatively poor acoustics performance at the target Reynolds number for small wind turbines in built environment.

2.1.2. Blade design

A section of a blade at radius r is illustrated together with the associated velocities, forces and angles in Figs. 3 and 4. The relative wind vector at radius r, denoted as W, is the resultant of an axial component U_P, and a rotational component U_T. The rotational component is the sum of the velocity due to the blades motion $r\Omega$, and the swirl velocity of the air $ra'\Omega$. The axial velocity U_P, is reduced by a component U_0a, due to the wake effect or blockage imposed by the blades, where U_0 is the upstream undisturbed wind speed. The a' and a terms represent the rotational and axial induction factors, respectively. The angle of attack is denoted by α, the pitch angle of the blade by θ, and the angle of the relative wind to the plane of rotation, by Φ. The resultant lift and drag forces are represented by L and D, and directed perpendicular and parallel to the relative wind as shown. The downstream wind speed is reduced down to $U_0(1\text{-}2a)$ because the turbine extracts energy from the wind (Fig. 4). Note that across the rotor disk, the angular velocity of the air relative to the blade increases from Ω to $\Omega\,(1+a')$ because of the wake rotation of the flow.

A FORTRAN code was developed in house by employing BEM method. Fig. 5 is the flow chart of this code,

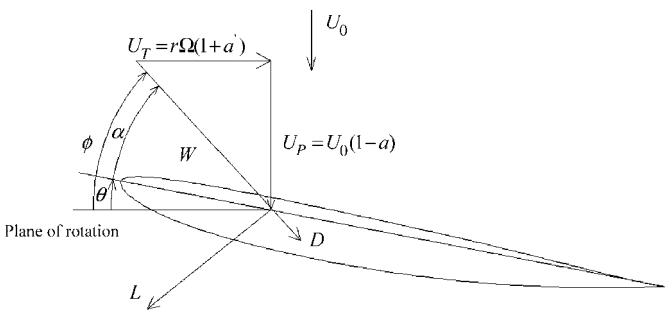

Fig. 3. Schematic diagram showing the section of a blade at radius r.

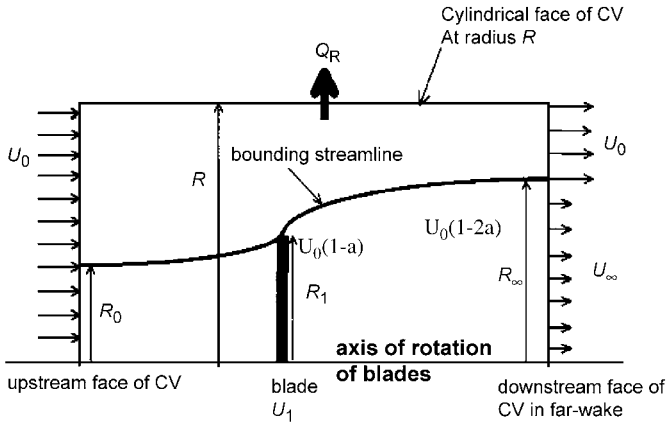

Fig. 4. A cross section of the flow through the rotor.

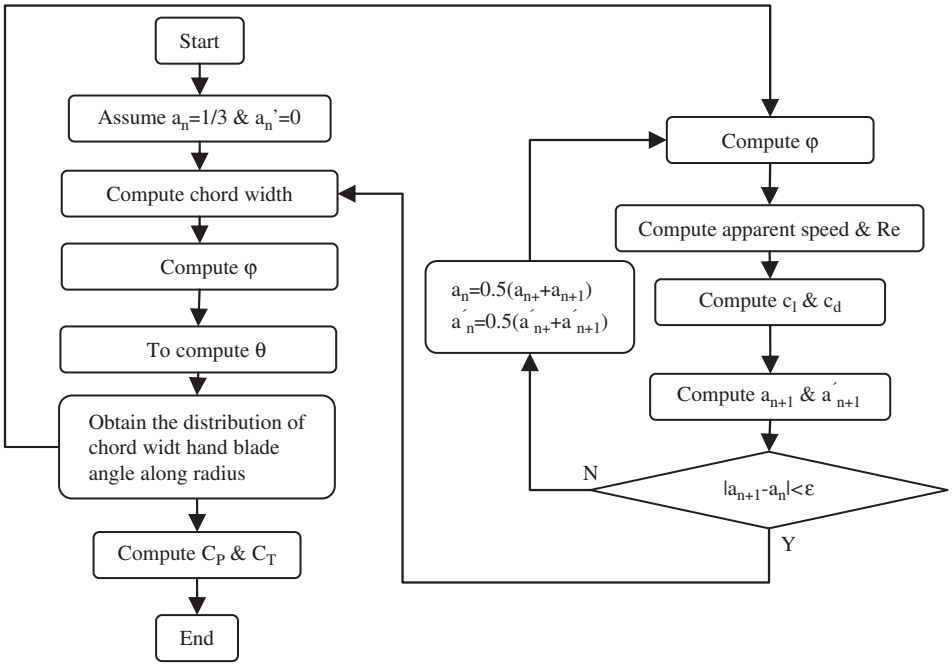

Fig. 5. Flowchart of the FORTRAN code for designing the blade

which consists of two parts. Part 1 is the rough design in which the blade shape was decided: the angle of relative wind and chord along the radius at *i*th section were decided by the following equations in the design code [17].

$$\varphi_i = (\tfrac{2}{3})\tan^{-1}(1/\lambda_{r,i}), \tag{1}$$

$$c_i = \frac{8\pi r_i}{BC_l}(1-\cos\varphi_i). \tag{2}$$

Part 2 in the flow chart is to compute the characteristics of rotor using the design code. Meanwhile Part 2 also gives some useful information to alter the draft design of Part 1. It is computed iteratively until a satisfied result is obtained. The procedure in flow chart begins with the choice of various rotor parameters and the choice of an airfoil. An initial blade shape is then determined using the blade element analysis assuming wake rotation. The final blade shape and performance are determined iteratively considering drag, tip losses, and ease of manufacture. The details of blade design can be found in [17] including the lift and drag coefficients used in this calculation.

Several control parameters need to be determined for an optimal blade design: the rated wind speed, U_0, the tip radius R_t and hub radius R_h, a tip speed ratio λ, the number of blades, a suitable airfoil for small wind turbine.

Normally a particular wind speed U_0 is assumed between 5–8 m s^{-1} depending on the design targets. Very often this is the rated speed. In this study, it was believed that the wind turbine should operate most efficiently at the wind speed that occurs most frequent during a year. Hence the free wind speed was 3.9 m s^{-1}. This figure was derived by Weibull fitting using the standard weather data prepared for heating and cooling design for buildings by Chartered Institution of Building Services Engineers[29]. This wind was raised to 5.7 m s^{-1}, using the acceleration rate inside the scoop predicted in the first part of this study.

The tip and hub diameters were decided according to the desired power output and the dimensions of the generator of the wind turbine. A tip speed ratio λ was chosen according to the length of the blades normally within the range from 3 to 6.

The effects of the scoop being considered so far were only the acceleration, although it was believed that the scoop should affect the airflow flow passing through the rotor. As the scoop confines the flow within itself, it should alter the normal bounding streamline of a rotor in open air, shown in Fig. 4. Therefore both a and a' would be smaller than normal. But the effects of the diffuser on the flow field were not examined in the blade design process, and were considered in the parameter study using CFD where the power yield of the actual combie, the rotor and scoop, was used as the criterion for its performance assessment.

2.2. Computational parametric study

The paper [19] details the ability of the CFD method to reveal flow details and compute power output of a rotor, and documents the systematic validation exercise on the method. The method was adopted here as a test platform, sometimes referred as virtual wind tunnel (Fig. 6), to carry out a series of tests in searching for the optimised rotor from various design options, including the connection method of the blades, the profile and dimension of nose cones and nacelle, distance of rotor in the scoop. The assessment criterion was the calculated power output of each of these options. As the mutual dependence of the

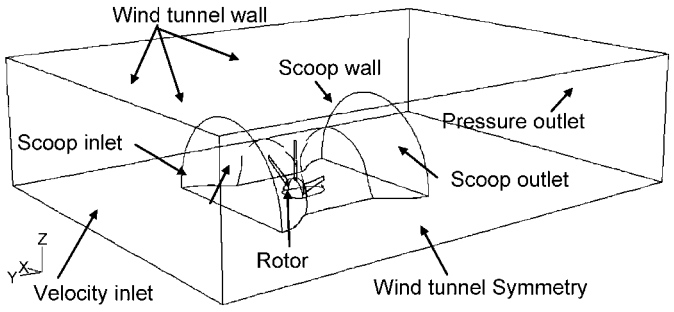

Fig. 6. Computational domain and boundary conditions of the CFD model, the virtual wind tunnel.

aerodynamic behaviour of the rotor and scoop required the study to be done through thorough and systematic tests, in each of these tests, only one parameter was varied to assess the effects of this parameter. These exercises would lead to determine the design configuration of the wind turbine that provides the greatest power output. The test procedure is detailed in Table 1, which includes eight modelling exercises the design options:

1. Two connection methods of blade (Options 1 and 2).
2. Four different profiles of noses and nacelles (Options 3–6).
3. Two sizes of the combined nose and nacelle (Options 6 and 7).
4. Two different positions of rotor inside the scoop. (Options 7 and 8).

In the models, the blade profiles with precise coordinates were created using a 3D CAD package (Rhinoceros) and then exported into the GAMBIT, a preprocessing program for CFD codes. The rest of the models including the scoop and the domain were finished and the whole domain was meshed in GAMBIT. A commercial CFD package, Fluent was used to do the modelling and calculate the power output of the wind turbine in the scoop and the flow field around the turbine was defined by the Reynolds averaged Navier–Stokes equations complemented by the RNG $k-\varepsilon$ turbulence model with standard wall functions.

A uniform velocity boundary condition was applied to the entrance of the domain, whilst the pressure outlet to the exit. The blades and hub were set as the rotational parts, of which the rotation speed could be defined by the tip ratio speed. Single reference frames (SRF) model was used to simulate the incompressible, steady-state flow field. The symmetrical boundary condition was assigned to the central cross section of the computational domain so that only half of the flow region was modelled in order to save computing costs (Fig. 7).

The dimension of the area perpendicular to the flow direction in the virtual wind tunnel was 4.5 times the diameter of the rotor in the axial direction, and was 3.6 times diameter of the rotor in the direction of cross section.

One of the major difficulties in CFD modelling was to mesh the flow domain near the rotor. The grid should be fine enough to capture the details of geometry and flow field at these spots, but not too large to handle by the available computing capacity. Fig. 8 shows the details of the mesh system created in the CFD model. The surface grid of the domain, the blades and hub are shown in Fig. 7(b)–7(c). Tetrahedral elements were used to mesh the domain since the geometry made up of the scoop and rotor was complicated. Three boundary layers meshes were added around the blades to simulate the turbulence flow in order to predict the pressure force and viscous force accurately (Fig. 7(c)). And size function was used near the zone of blades resulting in a mesh of 115 thousands cells.

A grid dependence study was done, which was a very time-consuming exercise, as each option needed computing over 3000 iterations for about over 1.4 million grids. Each case took more than 24 h of computation time with the fastest PC (Pentium 4 3.20GHz, RAM:1.12GB) available at the time when this study was carried out.

2.3. Annual power output calculation methods

A statistical analysis for a real wind data recorded in local station was carried out for two objectives: The first was to identify the rated wind speed that had highest frequency of occurrence. This speed was then used as rated speed for blade design, so that the rotor would be able to work more efficiently for more hours throughout a year. The second was to count the numbers of hours of the occurrence of consecutive wind speeds of a year. Annual energy yield is calculated by cumulating the productions of the number of hours and the power output over consecutive speeds.

The annual power output of a wind turbine has been always a figure directly showing its financial viability more than other technical features. Therefore a standard method of calculation is well established (Table 3) [30]. For micro, and small wind turbine, however, unlike the large wind turbines for which standards have been well established, the methods to calculate the power output have been found varying, resulting in a wide range of the predicted performance for similar size turbines [31]. Some simplest one even use the production of rated power output and total hours in a year, which gives very promising annual energy yield.

To illustrate the diversity in the prediction, three methods were applied in this study. All of them used the cumulated power generated at a consecutive wind speed bands from the cut in speed to the stop speed: standard method of calculating the annual power output was also used:

$$E_{\text{year}} = \sum_{V_{\text{start}}}^{V_{\text{stop}}} P(u) f(u) \times 8765,$$

where $P(u)$ is the power curve and $f(u)$ the possibility of occurrence of a wind speed.

In the first method, a real wind data recorded hourly in Edinburgh Airport was used for the $f(u)$. In the second,

Table 1
Nine modelling exercises with various design options

Options	Curves	Profiles	Equations	Parameters[a]	Power (w)
1			Original 913 nose cone without nacelle	CM = 1 DL = 600 mm	62.58
2			Original 913 nose cone without nacelle	CM = 2 DL = 600 mm	64.25
3	Parabola	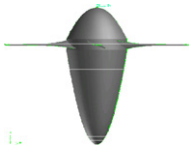	$y = \frac{D}{2}\left(1 - \frac{x}{L}\right)^P$	$D = 260.92$ mm, $F = 0$, $L = 391.38$ mm, $P = 0.5$ CM = 1, DL = 600 mm	43.86
4	Tangent ogive		$y = \frac{D}{2}\left(1 - \left(\frac{x+F}{L}\right)^P\right)\left(\frac{A^P}{A^P - F^P}\right)$	$D = 260.92$mm, $F = 0$, $L = 391.38$mm, $P = 0.5$ CM = 1, DL = 600 mm	47.05
5	Secant ogive	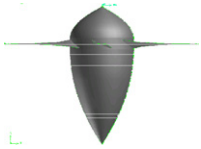	$y = \frac{D}{2}\left(1 - \left(\frac{x}{L}\right)^P\right)$	$D = 260.92$mm, $F = 3$, $L = 391.38$ mm, $P = 0.5$ CM = 1, DL = 600 mm	46.07
6	Ellipse	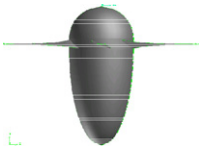	$y = \left(\left(\frac{D}{2}\right)^P\left(1 - \frac{x}{L}\right)^P\right)^{1/P}$	$D = 260.92$ mm, $F = 3$, $L = 391.38$ mm, $P = 0.5$ CM = 1, DL = 600 mm	49.09
7	Ellipse	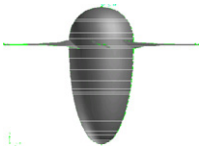	$y = \left(\left(\frac{D}{2}\right)^P\left(1 - \frac{x}{L}\right)^P\right)^{1/P}$	$D = 260.92$mm, $F = 3$, $L = 260.92$ mm, $P = 0.5$ CM = 1, DL = 600 mm	54.8
8	Ellipse	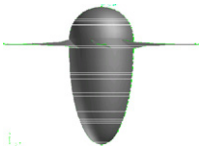	$y = \left(\left(\frac{D}{2}\right)^P\left(1 - \frac{x}{L}\right)^P\right)^{1/P}$	$D = 260.92$ mm, $F = 3$, $L = 260.92$ mm, $P = 0.5$ CM = 1, DL = 400mm	60.05

Parameters of the profile D and L: diameter and length of nose cone receptively; F: Offset; P: Power; CM: connection methods; DL: the distance of rotor position from the inlet of the scoop.

[a]Parameters of curves D and L represent diameter and length of nose cone, receptively; F represents offset; and P represents power.

these read wind data were used to fit into a Weibull distribution formula. The derived average speed of $3.8\,\mathrm{m\,s^{-1}}$ was used as the design wind speed in this exercise for blade design. In the third, the Weibull formula was used again for the $f(u)$. But this time, the standard n was 2, and the mean annual hourly wind speed at 10 m above ground level was $5.7\,\mathrm{m\,s^{-1}}$, which was calculated for Edinburgh using the standard method British Wind Energy Association.

For comparison, these methods were also applied to another two small wind turbines of the similar size.

In all the three methods, it was assumed that the rotor responded immediately to the changes of both speed and directions.

3. Results and discussions

3.1. Blades design

The basic rotor parameters are listed in Table 2. The rated wind speed was determined by the statistical wind data analysis, as explained above. Considering the flow

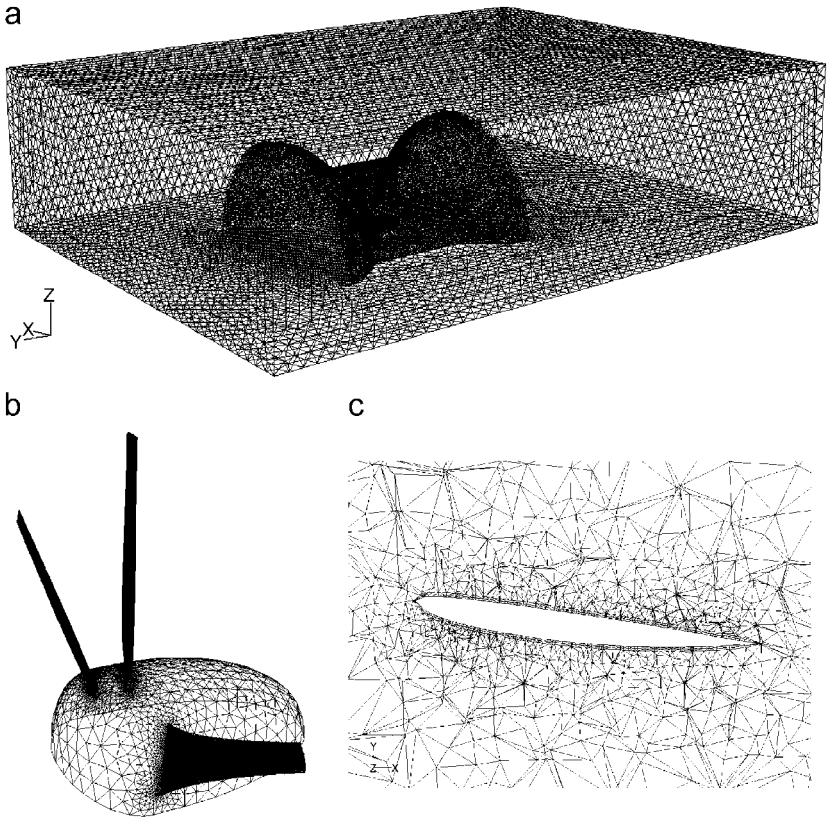

Fig. 7. Details of the mesh system created in the CFD model. (a) Mesh and geometry of the whole computational domain. (b) Mesh details around the rotor. (c) The mesh around the blade, details of the boundary layer surrounding the foil surface.

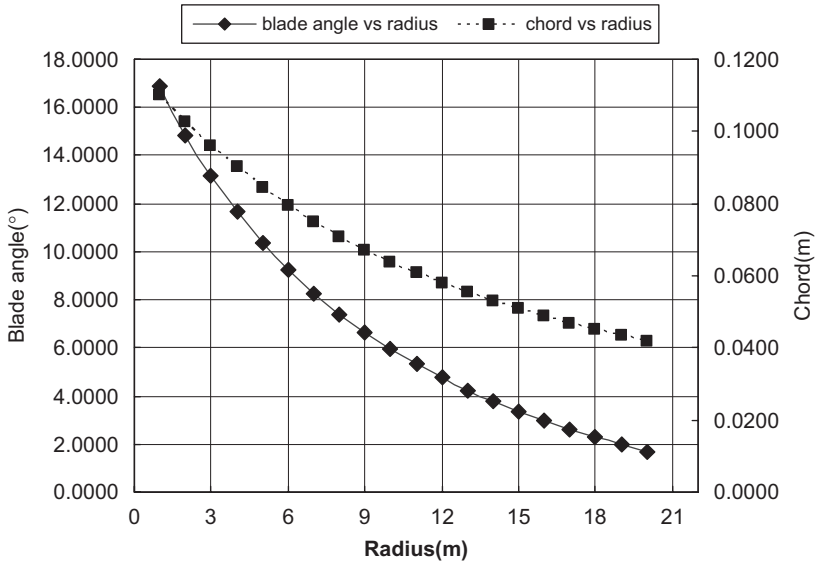

Fig. 8. Distributions of the blade angle and chord width respectively along the radius with wake rotation.

acceleration resulted from the scoop and nose cone, the final rated wind speed, measured at the rotor, was set to $5.7\,m\,s^{-1}$, 1.5 times of the prevailing wind speed taken into account of the speed augmentation inside the scoop.

Fig. 8 shows the blade angle and chord distributions along radius with wake rotation computed by the BEM method described above. The design with wake rotation took into account the generation of rotational kinetic energy in the wake, which resulted in less energy extraction by the rotor than it would be expected without wake rotation.

It has to pointed out that the blade was still not the optimised for at least two reasons. Firstly the lift and drag coefficients used in the BEM used quoted from the